

Received July 31, 2019, accepted August 9, 2019, date of publication August 22, 2019, date of current version September 4, 2019.

Digital Object Identifier 10.1109/ACCESS.2019.2936437

Joint Trajectory Design, Task Data, and Computing Resource Allocations for NOMA-Based and UAV-Assisted Mobile Edge Computing

XIANBANG DIAO¹, JIANCHAO ZHENG^{1,2}, YUAN WU^{3,4}, (Senior Member, IEEE),
YUEMING CAI¹, AND ALAGAN ANPALAGAN⁵, (Senior Member, IEEE)

¹College of Communications Engineering, Army Engineering University of PLA, Nanjing 210007, China

²National Innovation Institute of Defense Technology, Academy of Military Sciences of PLA, Beijing 100010, China

³State Key Laboratory of Internet of Things for Smart City, University of Macau, Taipa 999078, China

⁴Department of Computer and Information Science, University of Macau, Taipa 999078, China

⁵Department of Electrical and Computer Engineering, Ryerson University, Toronto, ON M5B 2K3, Canada

Corresponding author: Jianchao Zheng (longxingren.zjc.s@163.com)

This work was supported in part by the National Natural Science Foundation of China under Grant 61801505, in part by the Jiangsu Provincial Nature Science Foundation of China under Grant BK20170755, and in part by the National Postdoctoral Program for Innovative Talents of China under Grant BX201700109.

ABSTRACT Mobile edge computing (MEC) has been considered as a promising technique to address the explosively growing computation-intensive applications. Thanks to the flexibility of the unmanned aerial vehicles (UAVs), the UAV-assisted MEC can serve mobile terminals (MTs) effectively, i.e., the computing server installed on the UAV can flexibly change its location to serve MTs. Moreover, since non-orthogonal multiple access (NOMA) is able to accommodate massive connectivity, the NOMA-based and UAV-assisted MEC can provide flexible computing services for MTs in large-scale access networks (e.g., sensor networks and Internet of Things). However, due to the diversity of the UAV's trajectory and the interference among MTs introduced by NOMA, the performance (e.g., energy consumption and delay) of the NOMA-based and UAV-assisted MEC system is adversely affected. Therefore, in this paper, we formulate an optimization problem to minimize the largest energy consumption among MTs by jointly optimizing the trajectory, task data and computing resource allocations, and then propose an iterative algorithm to solve the optimization problem. Furthermore, to minimize the largest energy consumption among MTs with lower complexity, we propose a fixed point service scheme and optimize the location of the fixed point. The simulation results show that the proposed optimization algorithms can effectively reduce the largest energy consumption among MTs and ensure the fairness among MTs.

INDEX TERMS Mobile edge computing, non-orthogonal multiple access, unmanned aerial vehicles, trajectory design.

I. INTRODUCTION

The past decades have witnessed a significant growth in smart mobile applications such as face recognition, speech recognition, and virtual reality that enrich people's life [1]–[3]. However, these applications are usually computation-resource hungry and energy-consumption hungry, which however contradicts the reality that most

conventional mobile terminals (MTs) are constrained by limited computing-units and battery energy [4]. Thanks to allowing MTs to offload computing tasks to nearby computing servers, mobile edge computing (MEC) has been considered as a promising technology that can help MTs to undertake computing tasks [5]–[8].

Computing servers are traditionally deployed in the base stations. The fixed locations of the computing servers cannot cope with unexpected situations (e.g., base stations are damaged and environmental awareness is needed in disaster

The associate editor coordinating the review of this article and approving it for publication was Xiaodong Xu.

areas) and satisfy the needs of temporary computing services. To solve the problem, the flexible location deployment for computing servers is essential. Recently, unmanned aerial vehicles (UAVs) attract a lot of attentions due to their location-flexibility and maneuverability [9], [10]. According to the existing studies [11]–[15], the UAV can be quickly deployed as a platform over the air to satisfy urgent services. Thus, in MEC systems, the computing servers can be installed on the UAV and provide location-flexible computing services for the MTs in a wide area.

Moreover, the MEC is also needed in some large-scale access networks (e.g., the sensor networks and Internet of Things). However, traditional access protocols (e.g., time division multiple access (TDMA) and orthogonal frequency division multiple access (OFDMA)) cannot accommodate massive connectivity with high spectrum utilization. The power-domain non-orthogonal multiple access (NOMA) [16]–[20] allows multiple MTs to reuse the same time slot and frequency resource blocks by dividing their transmit power and further exploiting the successive interference cancellation to mitigate the co-channel interference among them. Because of the advantages of NOMA, NOMA-based MEC system can provide large-scale access and complete the computing offloading services in large-scale access networks [21]–[23].

A. RELATED WORK

The existing studies have recently investigated the UAV-assisted MEC systems. In [24] and [25], the authors used the effective alternative algorithm to solve the minimization problem of energy consumption and the maximization problem of computing rates in UAV-enabled wireless-powered MEC systems, respectively. In [26], the authors formulated a novel optimization framework for the utility maximization problem by jointly optimizing the transmit power of vehicle and the trajectory of UAV. In [27], the authors considered joint offloading and trajectory design for UAV-enabled MEC systems and aimed at minimizing the sum of the largest delay among users. In [28] and [29], the authors considered both uplink and down link in the system and minimized the sum of users' energy consumption by optimizing the bit allocation and path planning. However, the above studies do not consider the demand of large-scale access in the MEC system.

Moreover, the NOMA-based MEC systems have been recently studied. Specifically, some existing studies focus on the delay minimization. In [30], the authors studied the NOMA-enabled multi-access MEC system and aimed at optimizing the offloading tasks, the uploading and downloading durations to minimize the overall delay of the users. In [31], the authors proposed a social trust-based and cooperative computing offloading algorithm to minimize the completion delay of the system. Moreover, there are studies which focus on the energy consumption minimization. In [32], the authors proposed an edge computing aware NOMA technique and minimized the energy consumption of users.

In [33], the authors optimized the task partitions, power and offloading rates to minimize the weighted sum of the energy consumption for all users. In [34], a distributed scheme has been proposed for multi-user NOMA assisted multi-access MEC by jointly optimizing the users' offloaded workloads and the NOMA transmission-durations. However, the above studies do not consider the demand of urgent computing offloading services.

Different from the above existing studies, we consider the NOMA-based and UAV-assisted MEC system, which enables MEC to adapt to future scenarios requiring large-scale access and emergency deployment. To the authors' best knowledge, our paper is the first work which investigates the NOMA-based and UAV-assisted MEC system.

B. CHALLENGES AND CONTRIBUTIONS

In the NOMA-based and UAV-assisted MEC system, MTs upload their task data to the moving UAV with the NOMA protocol, and the results are then returned to MTs after their tasks are completed by the UAV. The UAV's dynamic trajectory determines the channel gain between the UAV and MTs, which yields a significant impact on MTs' energy consumptions. The NOMA protocol introduces interference among MTs, and random task data allocation may cause strong interferences among MTs (especially, when the amount of the uploaded task data is large), thereby increasing the MTs' energy consumptions. Moreover, the allocation of computing resources directly affects the computing delay. Under the fixed task time tolerance and transmit power, the allocation of computing resources also has an impact on MTs' energy consumptions.

Therefore, in this paper, we propose an iterative algorithm that jointly optimizes trajectory, task data and computing resource allocations to minimize the largest energy consumption among MTs. Furthermore, to design a low-complexity algorithm for minimizing the largest energy consumption among MTs, we propose a fixed point service scheme. In the considered fixed point scheme, the UAV only needs to hover at a fixed point to provide computing services, which thus reduces the complexity compared to the previous moving scheme providing a large number of service points. Regarding this low-complexity algorithm, we further optimize the location of the fixed point. The main contributions of the paper are summarized as follows.

- 1) First, we introduce the NOMA and UAV into MEC systems to meet the demand of urgent and large-scale access computing offloading services. On the one hand, the UAV can provide urgent computing offloading services. On the other hand, the NOMA can improve the number of accesses. Moreover, to ensure fairness and energy saving, we analyze the factors that influence MTs' energy (e.g., the interferences among MTs, the computing resource allocation strategy and the dynamic trajectory of the UAV) in the NOMA-based and UAV-assisted MEC system, and formulate a min-max problem of MTs' energy consumptions.

2) Next, we jointly optimize the trajectory, task data and computing resource allocations to solve the min-max problem (i.e., minimizing the largest energy consumption among MTs). The optimization problem is challenging due to the uncertainty of UAV's trajectory and the interference among MTs introduced by the NOMA protocol. We introduce auxiliary variables and utilize the structural characteristics of the optimization problem to transform it to convex sub-problems, and propose an iterative algorithm to effectively solve these sub-problems.

3) Furthermore, to solve the optimization problem with lower complexity, we propose a fixed point service scheme and find the optimal location of the fixed point. Specifically, we first utilize a closer approximation to deal with the interference in the location optimization, and mathematically prove that this approximation can help transform the original non-convex constraint into a convex constraint. Based on this, we transform the original non-convex optimization problem into a convex optimization problem and solve it efficiently.

Remark: Our design features are the introduction of NOMA and UAV into the MEC system for urgent and large-scale access computing offloading services. In addition, in order to ensure fairness and energy saving in the system, the largest energy consumption among MTs is minimized by jointly optimizing the UAV's trajectory, task data and computing resource allocations. Moreover, constraints include the MTs' task delay constraints, total amount of task data constraints, and the UAV's trajectory constraints, which will be discussed in detail in the next section. Our proposed design can yield a fairer optimization of MTs' energy consumptions while satisfying the demands of urgent and large-scale access computing offloading services.

C. PAPER ORGANIZATION

The rest of this paper is organized as follows. In Section II, we introduce the system model and formulate the optimization problem. In Section III, we propose an iterative algorithm to solve the optimization problem. In Section IV, a fixed point service scheme is proposed and we design a low-complexity algorithm to solve the optimization problem. Section V presents the numerical results. Finally, we conclude the paper in Section VI.

II. SYSTEM MODEL AND PROBLEM FORMULATION

A. SYSTEM MODEL

As shown in Fig. 1, we consider a wireless communication system where a rotary-wing UAV equipped with a computing server is dispatched to serve K MTs, denoted by $\mathcal{K} = \{1, 2, \dots, K\}$. Specifically, in a finite time horizon T , UAV provides computing services for MTs, and the task data are bit-wise independent and can be arbitrarily divided into different groups [1]. Moreover, the computing resources of the UAV are divided into f_{tot} computing resource blocks. For the convenience of analysis, T is divided into N equal time

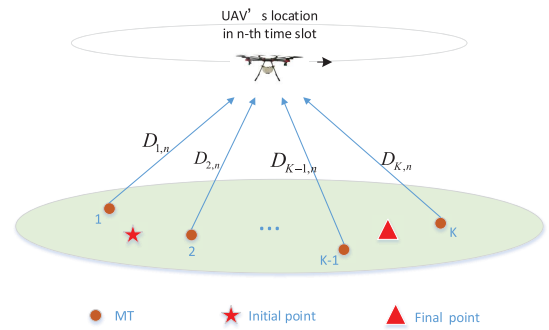


FIGURE 1. Illustrative scenario of NOMA-based and UAV-assisted computing offloading.

slots δ_t , i.e., $T = N\delta_t$, and denote $\mathcal{N} = \{1, 2, \dots, N\}$, when the δ_t is sufficiently small, the position of the UAV during each time slot can be regarded as stationary. In the n -th time slot, each MT k offloads the task $A_{k,n} \triangleq (D_{k,n}, X_{k,n})$ to the UAV in the NOMA protocol, where $D_{k,n}$ is the input-data size of the MT k in the n -th time slot (in bits) and $X_{k,n}$ represents the computing intensity which is assigned to the MT k in the n -th time slot (in the unit of CPU cycles per bit). We assume that the UAV flies at a constant altitude H and construct a 3-Dimensional Cartesian coordinate system model [25]–[27], where the coordinate of MT k is $\mathbf{w}_k = [x_k, y_k, 0]^T, \forall k \in \mathcal{K}$ and the coordinate of UAV in the n -th time slot is $\mathbf{q}_n = [x_{q,n}, y_{q,n}, H]^T$. The velocity of the UAV in the n -th time slot is \mathbf{v}_n . By taking into account the mobility constraints for the UAV's movement, we impose the following constraints:

$$C1: \begin{cases} \mathbf{q}_1 = \mathbf{q}_I, \\ \mathbf{q}_{N+1} = \mathbf{q}_F, \\ \mathbf{v}_n = \frac{\mathbf{q}_{n+1} - \mathbf{q}_n}{\delta_t}, \quad \forall n \in \mathcal{N}, \\ \|\mathbf{v}_n\| \leq V_{\max}, \quad \forall n \in \mathcal{N}, \end{cases} \quad (1)$$

where \mathbf{q}_I and \mathbf{q}_F are the initial and final locations of the UAV, respectively. V_{\max} is the maximum rate of the UAV, and $\|\cdot\|$ represents the norm operator. The above equations indicate that the initial and final locations of the UAV are fixed and show the relationship between the speed and position of the UAV.

Suppose that the UAV-to-ground channel is dominated by the line-of-sight link. Therefore, similar to [11]–[14], the channel gain between the UAV and the MT k in the n -th slot is given by:

$$g_{k,n} = \beta_0 \|\mathbf{q}_n - \mathbf{w}_k\|^{-2}, \quad (2)$$

where parameter β_0 represents the channel power at the reference distance $d_0 = 1$ m. We denote the transmit power of MT k in the n -th time slot as $p_{k,n}$. Without loss of generality, we assume that $g_{1,n} > g_{2,n} > \dots > g_{K,n}$. Based on the rules of the uplink power-domain NOMA [18], $p_{1,n} > p_{2,n} > \dots > p_{K,n}, \forall n \in \mathcal{N}$, and the decoding order of all MTs' signals in the UAV should be sorted in the ascending order of the MTs' sequence, namely, the signal of MT 1 with

largest channel gain is firstly decoded, and the signal of MT K with smallest channel gain is finally decoded. Moreover, according to the rule of successive interference cancellation (SIC) [18], the signal decoded previously is interfered by the signals decoded later. Thus, the transmission rate of the MT k in the n -th slot is given by:

$$R_{k,n} = B \log_2 \left(1 + \frac{p_{k,n} g_{k,n}}{\sum_{j=k+1}^K p_{j,n} g_{j,n} + \sigma^2} \right), \quad (3)$$

where parameters B and σ^2 are the channel bandwidth and noise power, respectively. Similar to [27], [32], the energy consumption and task delay of MT k in the n -th slot are respectively given by:

$$E_{k,n} = p_{k,n} \frac{D_{k,n}}{R_{k,n}}, \quad (4a)$$

$$T_{k,n} = \frac{D_{k,n}}{R_{k,n}} + \frac{X_{k,n} D_{k,n}}{f_{k,n} F}, \quad (4b)$$

where $f_{k,n}$ is the number of computing resources allocated to the MT k in the n -th time slot, and F is the computing rate of each computing resource (in the unit of CPU cycles per second). The delay $T_{k,n}$ includes the transmission delay $\frac{D_{k,n}}{R_{k,n}}$ and the computing delay $\frac{X_{k,n} D_{k,n}}{f_{k,n} F}$. It is worth noting that since the amount of computing results can be ignored compared to that of input data [27], [32], we do not consider the downlink delay.

B. PROBLEM FORMULATION

To ensure min-max fairness [35] among MTs, we aim to minimize the largest energy consumption among MTs by jointly optimizing the UAV's trajectory, task data and computing resource allocations, where the largest energy consumption refers to the energy consumption of the MT whose energy consumption is the largest among MTs. The optimization problem can be formulated as follows:

$$\mathbf{P1} : \min_{D_{k,n}, \mathbf{q}_n, f_{k,n}} \max_k \left\{ \sum_{n=1}^N E_{k,n} \right\}, \quad (5a)$$

$$\text{s.t. C1}, \quad (5b)$$

$$T_{k,n} \leq \delta_t, \quad \forall k \in \mathcal{K}, \forall n \in \mathcal{N}, \quad (5c)$$

$$\sum_{n=1}^N D_{k,n} = D_k^{\text{req}}, \quad \forall k \in \mathcal{K}, \quad (5d)$$

$$g_{1,n} > g_{2,n} > \dots > g_{K,n}, \quad \forall n \in \mathcal{N}, \quad (5e)$$

$$f_{k,n} \in \{f_{\min}, \dots, f_{\text{tot}} - (K-1)f_{\min}\}, \quad \forall k \in \mathcal{K}, n \in \mathcal{N}, \quad (5f)$$

$$\sum_{k=1}^K f_{k,n} = f_{\text{tot}}, \quad \forall n \in \mathcal{N}, \quad (5g)$$

where D_k^{req} is the required amount of task data of MT k . f_{\min} is the minimum number of computing resources allocated to each MT. Here, constraint (5b) represents the UAV's mobile

capacity constraints given in (1), constraint (5c) represents that all MTs' task delays in each time slot cannot exceed the length δ_t , constraint (5d) represents that constraint of task data, constraint (5e) ensures that under the NOMA protocol, all MT signals can be correctly decoded in the decoding order mentioned above. Constraint (5f) indicates that $f_{k,n}$ is an integer and cannot be lower than the minimum number of computing resource allocation or higher than the largest number of computing resource allocation. In addition, constraint (5g) indicates that the sum of the number of all MTs' computing resources is equal to the total amount of the UAV's computing resources.

Moreover, denote $i \in \mathcal{I} \triangleq \{1, \dots, K-1\}$ and $\mathcal{J}_i \triangleq \{i+1, \dots, K\}$, constraint (5e) can be rewritten as:

$$(2x_{q,n} - x_i - x_j)(x_i - x_j) + (2y_{q,n} - y_i - y_j)(y_i - y_j) > 0, \quad \forall i \in \mathcal{I}, \forall j \in \mathcal{J}_i, \forall n \in \mathcal{N}. \quad (6)$$

Obviously, the left-hand-side of (6) is affine with respect to \mathbf{q}_n . However, since the objective function and constraints (5c) are non-convex, the problem **P1** is a non-convex optimization problem and cannot be directly solved by the convex optimization techniques.

III. JOINT TRAJECTORY OPTIMIZATION AND TASK DATA ALLOCATION

In this section, we introduce auxiliary variables to transform the problem **P1** into a problem which can be solved efficiently. Firstly, we introduce the auxiliary variable $e \geq \max_k \left\{ \sum_{n=1}^N E_{k,n} \right\}$ to simplify the objective function and relax $f_{k,n}$ into a continuous number. Thus, the problem **P1** can be equivalently formulated as follows:

$$\mathbf{P2} : \min_{D_{k,n}, \mathbf{q}_n, f_{k,n}, e} e, \quad (7a)$$

$$\text{s.t. } e \geq \sum_{n=1}^N p_{k,n} \frac{D_{k,n}}{R_{k,n}}, \quad \forall k \in \mathcal{K}, \quad (7b)$$

$$\frac{D_{k,n}}{R_{k,n}} + \frac{X_{k,n} D_{k,n}}{f_{k,n} F} \leq \delta_t, \quad \forall k \in \mathcal{K}, \forall n \in \mathcal{N}, \quad (7c)$$

$$\sum_{n=1}^N D_{k,n} = D_k^{\text{req}}, \quad \forall k \in \mathcal{K}, \quad (7d)$$

$$f_{\min} \leq f_{k,n} \leq f_{\text{tot}} - (K-1)f_{\min}, \quad \forall k \in \mathcal{K}, n \in \mathcal{N}, \quad (7e)$$

$$\text{Constraint C1, (5g), (6)}, \quad (7f)$$

where constraint (7c) comes from constraint (5c). Moreover, since constraints (7b) and (7c) have the product terms of different variables, the problem **P2** is still intractable. To solve it, we introduce the auxiliary variables $t_{k,n} \geq \frac{1}{R_{k,n}}$. Therefore, constraints (7b) and (7c) can be equivalently rewritten as:

$$e \geq \sum_{n=1}^N p_{k,n} D_{k,n} t_{k,n}, \quad \forall k \in \mathcal{K}, \quad (8a)$$

$$D_{k,n}t_{k,n} + \frac{X_{k,n}D_{k,n}}{f_{k,n}F} \leq \delta_t, \quad \forall k \in \mathcal{K}, \forall n \in \mathcal{N}, \quad (8b)$$

$$R_{k,n} \geq \frac{1}{t_{k,n}}, \quad \forall k \in \mathcal{K}, \forall n \in \mathcal{N}, \quad (8c)$$

$$t_{k,n} > 0, \quad \forall k \in \mathcal{K}, \forall n \in \mathcal{N}. \quad (8d)$$

Since $R_{k,n}$ is non-concave with respect to \mathbf{q}_n , constraint (8c) is non-convex. Therefore, we define the following variables:

$$R_{k,n}^{\text{lb}} \triangleq B \log_2 \left(1 + \frac{p_{k,n}g_{k,n}}{\sum_{j=k+1}^K \frac{p_{j,n}\beta_0}{H^2} + \sigma^2} \right) < R_{k,n}, \quad \forall k \in \mathcal{K}, \forall n \in \mathcal{N}, \quad (9)$$

where $R_{k,n}^{\text{lb}}$ is still non-concave with respect to \mathbf{q}_n . Then, for any given local point $\mathbf{q}_n^{\text{local}}$ in the feasible domain, we define the following function:

$$R_k(\mathbf{q}_n) \triangleq B \log_2 \left(1 + \frac{a_{k,n}}{\|\mathbf{q}_n^{\text{local}} - \mathbf{w}_k\|^2 + H^2} \right) - \frac{Ba_{k,n} (\|\mathbf{q}_n - \mathbf{w}_k\|^2 - \|\mathbf{q}_n^{\text{local}} - \mathbf{w}_k\|^2)}{\ln 2 \left((\|\mathbf{q}_n^{\text{local}} - \mathbf{w}_k\|^2 + H^2)^2 + a_{k,n} (\|\mathbf{q}_n^{\text{local}} - \mathbf{w}_k\|^2 + H^2) \right)}, \quad (10)$$

where $a_{k,n} = \frac{p_{k,n}\beta_0}{\sum_{j=k+1}^K \frac{p_{j,n}\beta_0}{H^2} + \sigma^2} > 0$.

Theorem 2: For any \mathbf{q}_n in the feasible domain, we have $R_{k,n}^{\text{lb}} \geq R_k(\mathbf{q}_n)$.

Proof: We first define the function $f(x) \triangleq B \log_2 \left(1 + \frac{a_{k,n}}{x} \right)$, where $x > 0$. The first and second derivatives of function $f(x)$ are given by:

$$f'(x) = -\frac{Ba_{k,n}}{\ln 2 (x^2 + a_{k,n}x)}, \quad (11a)$$

$$f''(x) = \frac{Ba_{k,n} (2x + a_{k,n})}{\ln 2 (x^2 + a_{k,n}x)^2}. \quad (11b)$$

Since $f''(x) > 0$, $f(x)$ is a convex function. Therefore, according to the property of convex functions [35], we have $f(x) \geq f(y) - f'(y)(x - y)$, $\forall x, y > 0$. In addition, we define $x = \|\mathbf{q}_n - \mathbf{w}_k\|^2 + H^2$ and $y = \|\mathbf{q}_n^{\text{local}} - \mathbf{w}_k\|^2 + H^2$. Thus, we can obtain $R_{k,n}^{\text{lb}} \geq R_k(\mathbf{q}_n)$. ■

Therefore, constraint (8c) can be approximately transformed into the following inequality:

$$R_k(\mathbf{q}_n) \geq \frac{1}{t_{k,n}}, \quad \forall k \in \mathcal{K}, \forall n \in \mathcal{N}, \quad (12)$$

where $R_k(\mathbf{q}_n)$ is concave with respect to \mathbf{q}_n . Therefore, constraint (10) is convex with respect to \mathbf{q}_n and $t_{k,n}$. After the above operations, the problem **P2** can be formulated as:

$$\mathbf{P3} : \min_{D_{k,n}, \mathbf{q}_n, f_{k,n}, t_{k,n}, e} e, \quad (13a)$$

$$\text{s.t. } e \geq \sum_{n=1}^N p_{k,n}D_{k,n}t_{k,n}, \quad \forall k \in \mathcal{K}, \quad (13b)$$

$$R_k(\mathbf{q}_n) \geq \frac{1}{t_{k,n}}, \quad \forall k \in \mathcal{K}, \forall n \in \mathcal{N}, \quad (13c)$$

$$t_{k,n} > 0, \quad \forall k \in \mathcal{K}, \forall n \in \mathcal{N}, \quad (13d)$$

$$D_{k,n}t_{k,n} + \frac{X_{k,n}D_{k,n}}{f_{k,n}F} \leq \Delta, \quad \forall k \in \mathcal{K}, \forall n \in \mathcal{N}, \quad (13e)$$

$$\sum_{n=1}^N D_{k,n} = D_k^{\text{req}}, \quad \forall k \in \mathcal{K}, \quad (13f)$$

$$f_{\min} \leq f_{k,n} \leq f_{\text{tot}} - (K - 1)f_{\min}, \quad \forall k \in \mathcal{K}, n \in \mathcal{N}, \quad (13g)$$

$$\text{Constraint C1, (5g), (6)}. \quad (13h)$$

Although the problem **P3** is still non-convex, it can be transformed into different convex problems under different given variables. Specifically, we identify that problem **P3** can be decomposed into the following two subproblems:

- **Sub-problem to optimize the task data $D_{k,n}$ under given $\mathbf{q}_n, f_{k,n}$ and $t_{k,n}$.** The sub-problem can be formulated as:

$$\mathbf{P3.1} : \min_{D_{k,n}, e} e, \quad (14a)$$

$$\text{s.t. Constraints (13b), (13e), (13f)}. \quad (14b)$$

- **Sub-problem to optimize the trajectory \mathbf{q}_n , computing resources allocation $f_{k,n}$ and auxiliary variable $t_{k,n}$ under given $D_{k,n}$.** The sub-problem can be formulated as:

$$\mathbf{P3.2} : \min_{\mathbf{q}_n, f_{k,n}, t_{k,n}, e} e, \quad (15a)$$

$$\text{s.t. Constraints (13b) – (13e), (13g) – (13h)}. \quad (15b)$$

Algorithm 1 JTDCATO-Algorithm: Jointly Optimize Task Data and Computing Resource Allocations and Trajectory

- 1: Initialize $\{D_{k,n}, \mathbf{q}_n, f_{k,n}, t_{k,n}, e\}^0$ and set the iteration number $l = 0$, $\mathbf{q}_n^{\text{local}} = \mathbf{q}_n^0$ and the error tolerance $\varepsilon = 10^{-4}$
 - 2: **Repeat**
 - 3: Solve the problem **P3.1** with given $\{\mathbf{q}_n^l, f_{k,n}^l, t_{k,n}^l\}$ and obtain the optimal solutions $\{D_{k,n}^*\}$.
 - 4: Solve the problem **P3.2** with given $\{D_{k,n}^*\}$ and obtain the optimal solutions $\{\mathbf{q}_n^*, t_{k,n}^*, f_{k,n}^*, e^*\}$.
 - 5: Update $l \leftarrow l + 1$ and $\{D_{k,n}, \mathbf{q}_n, f_{k,n}, t_{k,n}, e\}^l \leftarrow \{D_{k,n}^*, \mathbf{q}_n^*, f_{k,n}^*, t_{k,n}^*, e^*\}$.
 - 6: **Until** $|e^l - e^{l-1}| \leq \varepsilon$
-

It can be verified that **P3.1** and **P3.2** are two convex optimization problems which can be solved via conventional optimization packages, e.g., CVX [36]. Similar to [37], we propose an iterative joint task data and computing

resource allocations and trajectory optimization algorithm (called JTDCATO-Algorithm) to solve the problem **P3**, and the JTDCATO-Algorithm is illustrated in Algorithm 1. In the JTDCATO-Algorithm, the first step is to obtain a feasible initial solution. The method for obtaining the initial solution is as follows. First, the allocation of task data is equally divided (i.e., $D_{k,n} = \frac{D_k^{req}}{N}, \forall k \in \mathcal{K}, n \in \mathcal{N}$). Next, for $f_{k,n}$, we allocate computing resources to each MT with the minimum number of computing resource allocation f_{min} . For the remaining computing resources, they can be randomly assigned to MTs. Then, the whole vertical bisectors of the line between any two MTs divide the whole horizontal plane into a number of areas, we take a line segment with two endpoints locating on the two edges of the area (i.e., the vertical bisectors that forms the area), and the line segment cannot exceed the area. Then, we determine the initial and final points of the UAV's trajectory on the line segment and divide the line segment between the initial and final points to equal N segments. Next, we determine the order of MTs based on the order of the distances from MTs to the UAV. Finally, we need to judge whether the trajectory satisfies constraints (5b) and (5c) or not. If constraints are satisfied, let $t_{k,n} = \frac{1}{R_{k,n}}, \forall k \in \mathcal{K}, n \in \mathcal{N}$ and set e to the largest energy consumption among MTs. If not, we reselect the two endpoints on the vertical bisectors and connect the two points to obtain a new straight trajectory satisfying the constraint of channel gain order until constraints (5b) and (5c) are satisfied. In addition, we use the rounding-off method to reconstruct the integral computing resource allocation variables, and based the integral computing resource allocation strategies, we use the JTDCATO-Algorithm again (since $f_{k,n}$ are already fixed, there is no need to optimize $f_{k,n}$ in the JTDCATO-Algorithm) to obtain the optimal trajectory and task data allocation strategies.

Moreover, the key idea of the JTDCATO-Algorithm is to iteratively optimize task data and computing resource allocations and UAV's flying trajectory. Each iteration is optimized on the basis of the previous iteration. Thus, when the iteration process continues, a series of non-increasing objective function values can be obtained. Meanwhile, the objective function of **P3** must be lower bounded by the optimal solution to the **P1**. Therefore, the convergence of the JTDCATO-Algorithm is guaranteed. Finally, regarding the complexity of our JTDCATO-Algorithm, since the JTDCATO-Algorithm requires alternatively solving the convex problems **P3.1** and **P3.2** which require polynomial complexities. Hence, the overall computation-complexity of JTDCATO-Algorithm is $O(I(KN)^3(2N + KN)^3)$ [38], where the I is the number of iterations. Recall that K denotes the number of MTs in the system, and N denotes the number of time slots.

IV. FIXED POINT SERVICE SCHEME

A. SCHEME DESCRIPTION AND PROBLEM FORMULATION

One of the effective ways to further reduce the computation-complexity of our JTDCATO-Algorithm is to simplify the trajectory of the UAV. Recently, there have been some studies

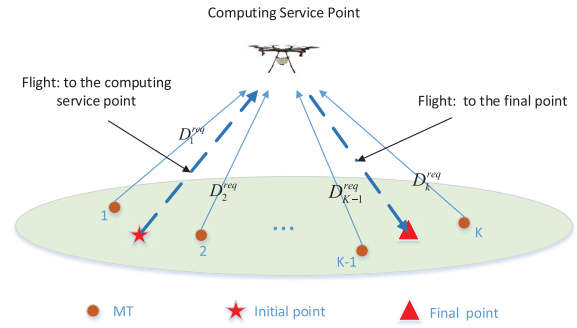


FIGURE 2. Illustrative scenario of the fixed point service scheme.

investigating the fixed point service (FPS) schemes. In [14] and [39], the authors assign several service points in consequence, and the UAV only needs to visit these service points and hover at these service points to provide services. Compared to the service scheme in which the UAV provides services while flying, the schemes in [14] and [39] can significantly reduce the total number of computing service points into a small number of computing service points, which significantly reduces the computational complexity. Based on this consideration, in this paper, we further propose a FPS scheme for the system.

As shown in Fig. 2, in a finite time horizon T , the UAV flies from the initial point \mathbf{q}_I to a computing service point \mathbf{q}_C (i.e., the fixed point) with the maximum rate, and hovers at \mathbf{q}_C to provide computing services for all MTs. After the computing tasks of all MTs are completed, the UAV flies to the final point \mathbf{q}_F with the maximum rate. During the period in which the UAV provides computing services, each MT k offloads the task data $A_k \triangleq (D_k^{req}, X_k)$ to the UAV using the NOMA protocol, where X_k represents the computing intensity which is assigned to the k -th MT during the service period (in the unit of CPU cycles per bit). We assume that the coordinate of the UAV's computing service point is $\mathbf{q}_C = [x_{qc}, y_{qc}, H]^T$, where H is a constant. We denote the transmit power of MT k as p_k . Similar to (2), the channel gain between the UAV and the MT k during the service period is given by:

$$g_k = \beta_0 \|\mathbf{q}_C - \mathbf{w}_k\|^{-2}, \quad (16)$$

and similar to [40], [41], we assume $g_1 > g_2 > \dots > g_K$ and $p_1 > p_2 > \dots > p_K$. Thus, the decoding order is the same as the decoding order described in the Section II. Moreover, the transmission rate of the MT k during the service period is given by:

$$R_k = B \log_2 \left(1 + \frac{p_k g_k}{\sum_{j=k+1}^K p_j g_j + \sigma^2} \right). \quad (17)$$

Similar to (4a)-(4b), the energy consumption and task delay of MT k during the service period are respectively given by:

$$E_k = p_k \frac{D_k^{req}}{R_k}, \quad (18a)$$

$$T_k^{task} = \frac{D_k^{req}}{R_k} + \frac{X_k D_k^{req}}{f_k F}, \quad (18b)$$

where f_k is the number of computing resources allocated to the MT k during the service period (in the unit of CPU cycles per second). Moreover, the flight delay of the UAV is related to the computing service point \mathbf{q}_C , and it can be given by:

$$T^{fly} = \frac{\|\mathbf{q}_C - \mathbf{q}_I\| + \|\mathbf{q}_C - \mathbf{q}_F\|}{V_{max}}. \quad (19)$$

To ensure the min-max fairness among MTs, we aim to minimize the largest energy consumption among MTs by optimizing the location of the UAV's computing service point and the computing resource allocation. The optimization problem can be formulated as follows:

$$\mathbf{P4}: \min_{\mathbf{q}_C, f_k} \max_k \{E_k\}, \quad (20a)$$

$$\text{s.t. } T_k^{task} + T^{fly} \leq T, \quad \forall k \in \mathcal{K}, \quad (20b)$$

$$g_1 > g_2 > \dots > g_K, \quad (20c)$$

$$f_k \in \{f_{min}, \dots, f_{tot} - (K-1)f_{min}\}, \quad \forall k \in \mathcal{K}, \quad (20d)$$

$$\sum_{k=1}^K f_k = f_{tot}. \quad (20e)$$

Constraint (20b) represents the sum of the task delay of any MT and the flight delay cannot exceed T , and constraint (20c) ensures that under the NOMA protocol, all MTs' signals are correctly demodulated at the UAV. Similar to (6), constraint (20c) can be rewritten as:

$$(2x_{qc} - x_i - x_j)(x_i - x_j) + (2y_{qc} - y_i - y_j)(y_i - y_j) > 0, \quad \forall i \in \mathcal{I}, j \in \mathcal{J}_i, \quad (21)$$

where the left-hand-side of (21) is affine with respect to \mathbf{q}_C . However, since the objective function and constraint (20b) are non-convex, this problem is still difficult to solve.

B. FIXED POINT OPTIMIZATION

In this subsection, we convert the problem **P4** into a convex problem by introducing auxiliary variables. Specifically, we introduce variable $e \geq E_k, \forall k \in \mathcal{K}$ and relax the f_k into a continuous number. Therefore, the problem **P4** can be equivalently written as:

$$\mathbf{P5}: \min_{\mathbf{q}_C, f_k, e}, \quad (22a)$$

$$\text{s.t. } e \geq E_k, \quad \forall k \in \mathcal{K}, \quad (22b)$$

$$T_k^{task} + T^{fly} \leq T, \quad \forall k \in \mathcal{K}, \quad (22c)$$

$$f_{min} \leq f_k \leq f_{tot} - (K-1)f_{min}, \quad \forall k \in \mathcal{K}, \quad (22d)$$

$$\text{Constraints (20e), (21)}. \quad (22e)$$

Since $\frac{1}{R_k}$ is non-convex with respect to \mathbf{q}_C , the problem **P5** is still non-convex. To handle it, we introduce variables $t_k \geq \frac{1}{R_k}$, and constraints (22b)-(22c) can be equivalently written as:

$$e \geq p_k D_k^{req} t_k, \quad \forall k \in \mathcal{K}, \quad (23a)$$

$$D_k^{req} t_k + \frac{X_k D_k^{req}}{f_k F} + \frac{\|\mathbf{q}_C - \mathbf{q}_I\| + \|\mathbf{q}_C - \mathbf{q}_F\|}{V_{max}} \leq T, \quad \forall k \in \mathcal{K}, \quad (23b)$$

$$R_k \geq \frac{1}{t_k}, \quad \forall k \in \mathcal{K}, \quad (23c)$$

$$t_k > 0, \quad \forall k \in \mathcal{K}. \quad (23d)$$

However, since R_k is non-concave with respect to \mathbf{q}_C , constraint (23c) is still non-convex. To solve this problem, we first rewrite the R_k as follows:

$$R_k = B \log_2 \left(\sum_{j=k}^K \frac{p_j \beta_0}{\|\mathbf{q}_C - \mathbf{w}_k\|^2 + H^2} + \sigma^2 \right) - B \log_2 \left(\sum_{j=k+1}^K \frac{p_j \beta_0}{\|\mathbf{q}_C - \mathbf{w}_k\|^2 + H^2} + \sigma^2 \right), \quad (24)$$

and then we introduce the following variables:

$$\alpha_k \leq \frac{1}{\|\mathbf{q}_C - \mathbf{w}_k\|^2 + H^2}, \quad \forall k \in \mathcal{K}, \quad (25a)$$

$$\alpha_k \geq 0, \quad \forall k \in \mathcal{K}, \quad (25b)$$

$$\exp(-\lambda_k) \geq \frac{1}{\|\mathbf{q}_C - \mathbf{w}_{k+1}\|^2 + H^2}, \quad \forall k \in \mathcal{K} \setminus \{K\}, \quad (25c)$$

where the α_k represents K variables and λ_k only represents $K-1$ variables. Since $\frac{1}{\|\mathbf{q}_C - \mathbf{w}_k\|^2 + H^2}$ and $\exp(-\lambda_k)$ are non-concave with respect to $\|\mathbf{q}_C - \mathbf{w}_k\|$ and λ_k , respectively, constraints (25a) and (25c) are non-convex. Then, constraints (25a) and (25c) can be rewritten as:

$$\|\mathbf{q}_C - \mathbf{w}_k\|^2 + H^2 \leq \frac{1}{\alpha_k}, \quad \forall k \in \mathcal{K}, \quad (26a)$$

$$\|\mathbf{q}_C - \mathbf{w}_{k+1}\|^2 + H^2 \geq \exp(\lambda_k), \quad \forall k \in \mathcal{K} \setminus \{K\}. \quad (26b)$$

Since $\frac{1}{\alpha_k}$ and $\|\mathbf{q}_C - \mathbf{w}_k\|^2$ are convex with respect to α_k and \mathbf{q}_C , respectively, for any given local point α_k^{local} and $\mathbf{q}_C^{\text{local}}$, we have:

$$\frac{1}{\alpha_k} \geq \frac{1}{\alpha_k^{\text{local}}} - \frac{1}{(\alpha_k^{\text{local}})^2} (\alpha_k - \alpha_k^{\text{local}}), \quad (27a)$$

$$\|\mathbf{q}_C - \mathbf{w}_{k+1}\|^2 \geq \left\| \mathbf{q}_C^{\text{local}} - \mathbf{w}_{k+1} \right\|^2 + 2 \left(\mathbf{q}_C^{\text{local}} - \mathbf{w}_{k+1} \right)^T \left(\mathbf{q}_C - \mathbf{q}_C^{\text{local}} \right), \quad (27b)$$

and the right-hand-sides of (27a) and (27b) are affine with respect to α_k and \mathbf{q}_C , respectively. Moreover, constraints (26a) and (26b) can be rewritten as:

$$\|\mathbf{q}_C - \mathbf{w}_k\|^2 + H^2 \leq \frac{1}{\alpha_k^{\text{local}}} - \frac{1}{(\alpha_k^{\text{local}})^2} (\alpha_k - \alpha_k^{\text{local}}), \quad \forall k \in \mathcal{K}, \quad (28a)$$

$$\left\| \mathbf{q}_C^{\text{local}} - \mathbf{w}_{k+1} \right\|^2 + 2 \left(\mathbf{q}_C^{\text{local}} - \mathbf{w}_{k+1} \right)^T \left(\mathbf{q}_C - \mathbf{q}_C^{\text{local}} \right) + H^2 \geq \exp(\lambda_k), \quad \forall k' \in \mathcal{K} \setminus \{K\}. \quad (28b)$$

In addition, we define variables as follows:

$$R_k^{\text{lb}} \triangleq B \log_2 \left(\sum_{j=k}^K p_j \beta_0 \alpha_j + \sigma^2 \right)$$

$$-B \log_2 \left(\sum_{j=k+1}^K p_j \beta_0 \exp(-\lambda_{j-1}) + \sigma^2 \right) \leq R_k, \quad \forall k \in \mathcal{K}, \quad (29)$$

where the subtractor of R_k^{lb} is a log-sum-exp formula which is convex [42]. Then, we define a series of functions as follows:

$$f_k(\alpha_k, \dots, \alpha_K) = B \log_2 \left(\sum_{j=k}^K p_j \beta_0 \alpha_j + \sigma^2 \right), \quad \forall k \in \mathcal{K}. \quad (30)$$

Theorem 3: For $\forall k \in \mathcal{K}$, $f_k(\alpha_k, \dots, \alpha_K)$ is a concave function.

Proof: We first define variables $o, u \in \{k, \dots, K\}$, $k \in \mathcal{K}$ and obtain the first partial derivative with respect to α_o as follows:

$$\frac{\partial f_k(\alpha_k, \dots, \alpha_K)}{\partial \alpha_o} = \frac{B\beta_0 p_o}{\ln 2 \left(\sum_{j=k}^K p_j \beta_0 \alpha_j + \sigma^2 \right)}. \quad (31)$$

Based on (31), we can obtain the second mixed partial derivatives with respect to α_o and α_u as follows:

$$\frac{\partial^2 f_k(\alpha_k, \dots, \alpha_K)}{\partial \alpha_o \partial \alpha_u} = -\frac{B\beta_0^2 p_o p_u}{\ln 2 \left(\sum_{j=k}^K p_j \beta_0 \alpha_j + \sigma^2 \right)^2}. \quad (32)$$

Therefore, we can obtain the Hessian matrix of $f_k(\alpha_k, \dots, \alpha_K)$:

$$\mathbf{H}_k = \gamma \begin{bmatrix} p_k^2 & p_k p_{k+1} & \cdots & p_k p_K \\ p_k p_{k+1} & p_{k+1}^2 & \cdots & p_{k+1} p_K \\ \vdots & \vdots & \ddots & \vdots \\ p_k p_K & p_{k+1} p_K & \cdots & p_K^2 \end{bmatrix}, \quad (33)$$

where $\gamma = -\frac{B\beta_0^2}{\ln 2 \left(\sum_{j=k}^K p_j \beta_0 \alpha_j + \sigma^2 \right)^2} < 0$. Furthermore,

we define:

$$\mathbf{H}'_k = \begin{bmatrix} p_k^2 & p_k p_{k+1} & \cdots & p_k p_K \\ p_k p_{k+1} & p_{k+1}^2 & \cdots & p_{k+1} p_K \\ \vdots & \vdots & \ddots & \vdots \\ p_k p_K & p_{k+1} p_K & \cdots & p_K^2 \end{bmatrix}. \quad (34)$$

Let $\mathbf{H}'_k(s-k+1, :) = \mathbf{H}'_k(s-k+1, :) - \frac{p_s}{p_k} \mathbf{H}'_k(1, :)$, $\forall s$, where $s \in \{k+1, \dots, K\}$. Then, we can obtain:

$$\mathbf{H}'_k = \begin{bmatrix} p_k^2 & p_k p_{k+1} & \cdots & p_k p_K \\ 0 & 0 & \cdots & 0 \\ \vdots & \vdots & \ddots & \vdots \\ 0 & 0 & \cdots & 0 \end{bmatrix}. \quad (35)$$

Thus, the $(K-k+1)$ -order principal minor of the \mathbf{H}'_k is:

$$\mathbf{D}_{K-k+1} = \begin{vmatrix} p_k^2 & p_k p_{k+1} & \cdots & p_k p_K \\ 0 & 0 & \cdots & 0 \\ \vdots & \vdots & \ddots & \vdots \\ 0 & 0 & \cdots & 0 \end{vmatrix} = 0. \quad (36)$$

Similarly, we can know that principal minors of arbitrary order of the \mathbf{H}'_k equal 0. Therefore, for $\forall k \in \mathcal{K}$, the \mathbf{H}'_k is a semi-positive matrix. Moreover, because of $\gamma < 0$, the Hessian matrix \mathbf{H}_k is a semi-negative matrix. Therefore, the $f_k(\alpha_k, \dots, \alpha_K)$ is a concave function. ■

In summary, R_k^{lb} is concave with respect to α_k and λ_k . After the above operation, the problem **P5** can be rewritten as:

$$\mathbf{P6} : \min_{\mathbf{q}_C, f_k, t_k, \alpha_k, \lambda_k, e} e, \quad (37a)$$

$$\text{s.t. } e \geq p_k D_k^{\text{req}} t_k, \quad \forall k \in \mathcal{K}, \quad (37b)$$

$$D_k^{\text{req}} t_k + \frac{X_k D_k^{\text{req}}}{f_k F} + \frac{\|\mathbf{q}_C - \mathbf{q}_I\| + \|\mathbf{q}_C - \mathbf{q}_F\|}{V_{\max}} \leq T, \quad \forall k \in \mathcal{K}, \quad (37c)$$

$$R_k^{\text{lb}} \geq \frac{1}{t_k}, \quad \forall k \in \mathcal{K}, \quad (37d)$$

$$t_k > 0, \quad \forall k \in \mathcal{K}, \quad (37e)$$

$$\alpha_k \geq 0, \quad \forall k \in \mathcal{K}, \quad (37f)$$

$$f_{\min} \leq f_k \leq f_{\text{tot}} - (K-1)f_{\min}, \quad \forall k \in \mathcal{K}, \quad (37g)$$

$$\text{Constraint (20e), (21), (28a) - (28b)}. \quad (37h)$$

Obviously, the problem **P6** is a convex problem and we propose a fixed point service algorithm (called FPS-Algorithm) to solve the problem **P6**. The FPS-Algorithm is illustrated in Algorithm 2 below. The FPS-Algorithm requires a polynomial complexity of $O((3K+1)^3)$ for solving the problem **P6**, which thus is lower than the complexity of the previous JTDCATO-Algorithm. In addition, we use the rounding-off method to reconstruct the integral computing resource allocation variables, and based the integral computing resource allocation strategies, we use the FPS-Algorithm again (since f_k are already fixed, there is no need to optimize f_k in the FPS-Algorithm) to obtain the optimal hover point.

Algorithm 2 FPS-Algorithm

- 1: Initialize $\mathbf{q}_C^{\text{local}}$ and α_k^{local} .
- 2: Solve the problem **P6** by CVX tool.
- 3: **Output:** \mathbf{q}_C^*, f_k^* .

V. NUMERICAL RESULTS

In this section, simulation results are presented to demonstrate the effectiveness of our proposed JTDCATO-Algorithm and FPS-Algorithm. There are $K = 4$ MTs with the respective positions of $\mathbf{w}_1 = (-100, 0, 0)$, $\mathbf{w}_2 = (100, 0, 0)$, $\mathbf{w}_3 = (-100, 200, 0)$, and $\mathbf{w}_4 = (100, 200, 0)$ in the system. Moreover, based on the typical settings in [21] and [27], we set other related system parameters as follows: $N = 150$, $T = 30$ s, $B = 1$ MHz, $V_{\max} = 30$ m/s, $\beta_0 = -50$ dB, $f_{k,n} = 1.2$ Gcps, $f_{\min} = 1$, $f_{\text{tot}} = 8$, and $\sigma^2 = -110$ dBm. According to 3GPP Release 15 [44], in order to ensure the existence of pure LoS, we set the UAV's altitude $H = 100$ m. In addition, we refer to the scheme of serving during the whole flight in the Section II as a general scheme. For the general scheme, $p_{1,n} = 0.1$ W, and $p_{k+1,n} = 0.9p_{k,n}$, $\forall k \in \mathcal{K}/\{K\}$, $n \in \mathcal{N}$. Similarly, for the FPS scheme,

$p_1 = 0.1$ W, and $p_{k+1} = 0.9p_k, \forall k \in \mathcal{K}/\{K\}$. Moreover, similar to [27] and [29], we make the following definitions: straight flight with uniform task data allocation is called “without (w.o.) opt” for the general scheme, and randomly selected computing service point is called “w.o. opt” for the FPS scheme. In addition, we regard the optimization algorithm in [43] as the benchmark algorithm and compare the proposed algorithm with it below. In addition, since the system model can be modeled as a simple mathematical model, we chose MATLAB as the simulation platform.

In Fig. 3, we show the required number of iterations of the JTDCATO-Algorithm versus the largest energy consumption among MTs. It can be observed from Fig. 3 that even at different altitudes, the JTDCATO-Algorithm can reach the convergence state within 15 iterations. In addition, we find that when the altitude becomes larger, the optimal largest energy consumption among MTs becomes smaller. This is mainly because when the altitude becomes larger, the interference among different MTs becomes smaller, which results in an increase in rate and a decrease in the largest energy consumption among MTs.

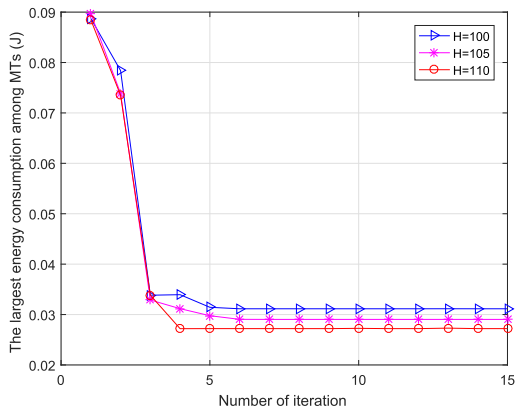


FIGURE 3. Iteration of the JTDCATO-Algorithm at different altitudes, with $D_k^{req} = 100\text{kbits}, \forall k \in \mathcal{K}$.

Fig. 4 shows the largest energy consumption among MTs versus the largest transmit power among MTs. As mentioned above, the transmit powers of all MTs are proportional. In order to satisfy the proportion relation of all MTs’ transmit powers, when the maximum transmit power among MTs changes, the transmit power of other MTs also changes. It can be seen from the figure that as the MTs’ transmit powers increase, the largest energy consumption among MTs shows an increasing trend. Moreover, our proposed JTDCATO-Algorithm and FPS-Algorithm always outperform the “w.o. opt.” algorithm and the largest energy consumptions among MTs obtained by our proposed algorithms are always smaller than those obtained by the benchmark algorithm. This result validates the superior performance of our proposed algorithm. In addition, with the increase of MTs’ transmit powers, the gap between our proposed algorithms and the “w.o. opt.” algorithm increases, which indicates that the proposed algorithm can achieve

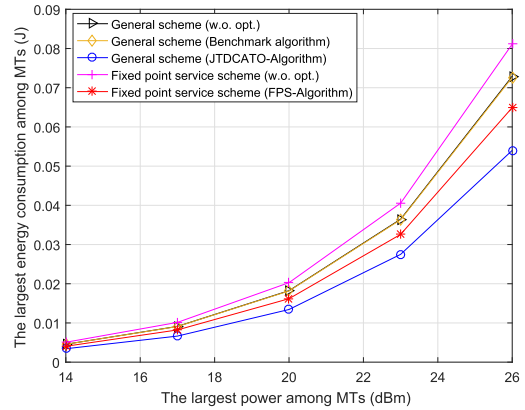


FIGURE 4. The largest energy consumption versus the largest transmit power among MTs, with $H = 100\text{m}, D_k^{req} = 100\text{kbits}, \forall k \in \mathcal{K}$.

greater performance gain when the MTs’ transmit power increase.

Fig. 5 presents the largest energy consumptions among MTs obtained by different algorithms under different required amount of task data. We can note that the largest energy consumption among MTs obtained by JTDCATO-Algorithm is the smallest among all algorithms in Fig. 5, which indicates the effectiveness of the JTDCATO-Algorithm. However, the JTDCATO-Algorithm requires a high complexity, which reduces the timeliness. The largest energy consumption among MTs obtained by the FPS scheme (FPS-Algorithm) is slightly greater than that obtained by the general scheme (JTDCATO-Algorithm), but only needs to solve a convex problem and does not require iterations. At the same time, the performance of the two proposed algorithms is better than other algorithms under the same scheme. In particular, our proposed algorithms are superior to the benchmark algorithm. Moreover, the performance of the benchmark algorithm is only slightly better than the “w.o. opt.” algorithm, which shows that the benchmark algorithm is not applicable for solving our problem. In addition, for general scheme, “Only data opt.” yields better results, while “Only trajectory opt.” even cannot outperform than the FPS scheme (w.o. opt.). This is because only optimizing one parameter in the approximated problem **P3** once cannot

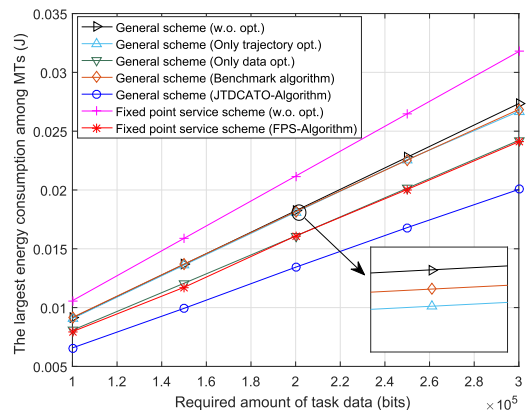


FIGURE 5. The largest energy consumption.

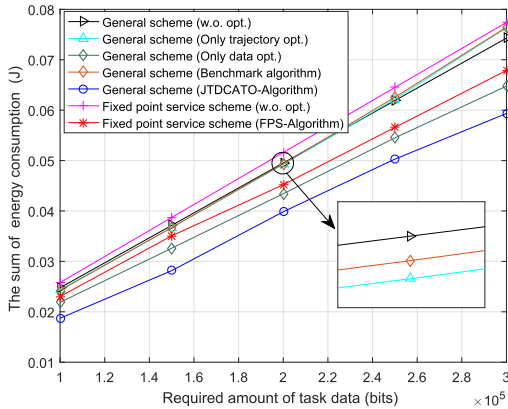


FIGURE 6. The sum of energy consumption.

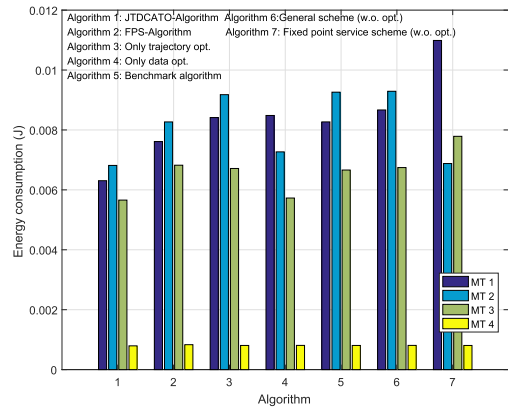


FIGURE 7. The energy consumption, with $D_k^{req} = 100\text{kbits}, \forall k \in \mathcal{K}$.

ensure that the original solution can be optimized. Therefore, in order to get better results, iterative optimization is needed, just like the JTDCATO-Algorithm.

Fig. 6 presents the sum of energy consumption under different required amount of task data. It can be seen from the figure that the sums of the energy consumption obtained by the two proposed algorithms are smaller than other algorithms under the same scheme. In addition, we observe that the sum of the energy consumption obtained by general scheme (JTDCATO-Algorithm) is also the smallest, which reflects that the general scheme (JTDCATO-Algorithm) can not only ensure fairness among MTs, but also has better global performance. However, the sum of the energy consumption obtained by the FPS scheme (FPS-Algorithm) is higher than that of general scheme (Only data opt.), which indicates that although the FPS scheme (FPS-Algorithm) can obtain preferable fairness among MTs, the global performance is inferior.

In addition, by comparing the Fig. 5 and Fig. 6, we observe that the largest energy consumption among MTs and the sum of energy consumption are basically linear with the required amount of task data. To reduce the MTs' energy consumptions, MTs upload task data in the time slots when the UAV is close to themselves, which makes MTs upload task data at roughly the same rate in these time slots. Moreover, the transmit powers of MTs are fixed, and combined with formula (4a), we can know that the MTs' energy consumptions are linear with the required amount of task data. Moreover,

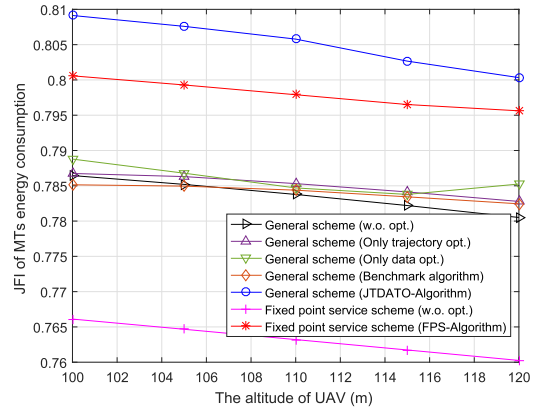


FIGURE 8. The JFI of MTs' energy consumptions, with $D_k^{req} = 100\text{kbits}, \forall k \in \mathcal{K}$.

we find that for the largest energy consumption among MTs and the sum of energy consumption, the gap between the general scheme (w.o. opt.) and general scheme (JTDCATO-Algorithm) is larger than the gap between the FPS scheme (w.o. opt.) and FPS scheme (FPS-Algorithm). This shows that optimization is more effective for the general scheme. In general, the general scheme (JTDCATO-Algorithm) can obtain the best performance, but the time complexity is relatively large. Compared with the general scheme (JTDCATO-Algorithm), the FPS scheme (FPS-Algorithm) can obtain sub-optimal performance, and the complexity is reduced. Thus, we can choose from the two schemes according to the practical needs.

Fig. 7 presents the energy consumption of all MTs obtained by proposed schemes and algorithms. It can be seen from Fig. 7 that the energy consumptions of MT 4 of different algorithms are roughly the same. As mentioned above, since MT 4 is not affected by other MTs, the impact of trajectory and task data allocation is weakened for MT 4. For MT 1-MT 3, we find that for the two schemes, the energy consumptions of MT 1-MT 3 under "w.o. opt." are quite different. Compared with the "w.o. opt." and the benchmark algorithm, our proposed optimization algorithms can greatly reduce the gap among MT 1-MT 3. This reflects that our proposed algorithm can ensure fairness among MTs. However, "Only trajectory opt." and "Only data opt." also cannot reduce the gap of energy consumption between MT 1-MT 3, which also indicates that for the general scheme, only optimizing one parameter in the approximated problem **P3** cannot ensure fairness among MTs.

Moreover, Fig. 8 shows the Jain's fairness index (JFI) [45] for MT's energy consumption under different algorithms. It can be seen from the figure that for the two schemes, the JFI of our proposed algorithms is higher than other algorithms as illustrated in the figure, which also shows that our proposed algorithms can enhance the fairness among MTs. In addition, as flying altitude of the UAV increases, the JFIs of all algorithms illustrated in the figure show downward trend, which indicates that increasing in H decreases the fairness among MTs.

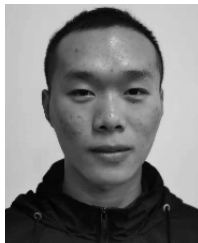
VI. CONCLUSION

In this paper, we have studied the NOMA-based and UAV-assisted MEC system. Two schemes have been investigated in the system, namely, the general scheme and the FPS scheme. For the general scheme, we have adopted the joint trajectory, task data and computing resource allocations optimization to minimize the largest energy consumption among MTs. We have solved the original non-convex problem by adding auxiliary variables and transforming it into two convex problems, which are solved iteratively. Moreover, to minimize the largest energy consumption among MTs with lower complexity, we have proposed the FPS scheme and optimized the location of the fixed point. The simulation results have showed that for both schemes, our proposed algorithms can effectively reduce the largest energy consumption among the MTs. In addition, compared with other algorithms as illustrated in the simulation section, our proposed algorithms can guarantee the fairness among MTs. In the future work, we will use event-driven software to model more realistic channel models for making the results more convincing.

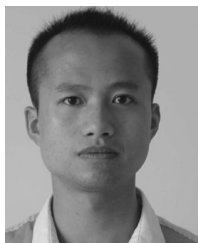
REFERENCES

- [1] Y. Xu and S. Mao, "A survey of mobile cloud computing for rich media applications," *IEEE Wireless Commun.*, vol. 20, no. 3, pp. 46–53, Jun. 2013.
- [2] S. Abolfazli, Z. Sanaei, E. Ahmed, A. Gani, and R. Buyya, "Cloud-based augmentation for mobile devices: Motivation, taxonomies, and open challenges," *IEEE Commun. Surveys Tuts.*, vol. 16, no. 1, pp. 337–368, Feb. 2014.
- [3] R. Li, Z. Zhao, X. Zhou, G. Ding, Y. Chen, Z. Wang, and H. Zhang, "Intelligent 5G: When cellular networks meet artificial intelligence," *IEEE Wireless Commun.*, vol. 24, no. 5, pp. 175–183, Oct. 2017.
- [4] J. Zheng, Y. Cai, Y. Wu, and X. Shen, "Dynamic computation offloading for mobile cloud computing: A stochastic game-theoretic approach," *IEEE Trans. Mobile Comput.*, vol. 18, no. 4, pp. 771–786, Apr. 2018.
- [5] Y. Mao, C. You, J. Zhang, K. Huang, and K. B. Letaief, "A survey on mobile edge computing: The communication perspective," *IEEE Commun. Surveys Tuts.*, vol. 19, no. 4, pp. 2322–2358, 4th Quart., 2017.
- [6] P. Mach and Z. Becvar, "Mobile edge computing: A survey on architecture and computation offloading," *IEEE Commun. Surveys Tuts.*, vol. 19, no. 3, pp. 1628–1656, 3rd Quart., 2017.
- [7] S. Wang, X. Zhang, Y. Zhang, L. Wang, J. Yang, and W. Wang, "A survey on mobile edge networks: Convergence of computing, caching and communications," *IEEE Access*, vol. 5, pp. 6757–6779, 2017.
- [8] S. Barbarossa, S. Sardellitti, and P. D. Lorenzo, "Communicating while computing: Distributed mobile cloud computing over 5G heterogeneous networks," *IEEE Signal Process. Mag.*, vol. 31, no. 6, pp. 45–55, Nov. 2014.
- [9] L. Gupta, R. Jain, and G. Vaszkun, "Survey of important issues in UAV communication networks," *IEEE Commun. Surveys Tuts.*, vol. 18, no. 2, pp. 1123–1152, 2nd Quart., 2016.
- [10] H. Shakhathreh, A. H. Sawalmeh, A. Al-Fuqaha, Z. Dou, E. Almaita, I. Khalil, N. S. Othman, A. Khreishah, and M. Guizani, "Unmanned aerial vehicles (UAVs): A survey on civil applications and key research challenges," *IEEE Access*, vol. 7, pp. 48572–48634, 2019.
- [11] Y. Zeng and R. Zhang, "Energy-efficient UAV communication with trajectory optimization," *IEEE Trans. Wireless Commun.*, vol. 16, no. 6, pp. 3747–3760, Jun. 2017.
- [12] Q. Wu, Y. Zeng, and R. Zhang, "Joint trajectory and communication design for multi-UAV enabled wireless networks," *IEEE Trans. Wireless Commun.*, vol. 17, no. 3, pp. 2109–2121, Mar. 2018.
- [13] C. Zhan, Y. Zeng, and R. Zhang, "Energy-efficient data collection in UAV enabled wireless sensor network," *IEEE Wireless Commun. Lett.*, vol. 7, no. 3, pp. 328–331, Jun. 2018.
- [14] Y. Zeng, J. Xu, and R. Zhang, "Energy minimization for wireless communication with rotary-wing UAV," *IEEE Trans. Wireless Commun.*, vol. 18, no. 4, pp. 2329–2345, Apr. 2019.
- [15] B. Li, Z. Fei, and Y. Zhang, "UAV communications for 5G and beyond: Recent advances and future trends," *IEEE Internet Things J.*, vol. 6, no. 2, pp. 2241–2263, Apr. 2019. doi: 10.1109/JIOT.2018.2887086.
- [16] Z. Ding, Y. Liu, J. Choi, Q. Sun, M. Elkashlan, C. L. I, and H. Poor, "Application of non-orthogonal multiple access in LTE and 5G networks," *IEEE Commun. Mag.*, vol. 55, no. 2, pp. 185–191, Feb. 2017.
- [17] H. Huang, J. Xiong, J. Yang, G. Gui, and H. Sari, "Rate region analysis in a full-duplex-aided cooperative nonorthogonal multiple-access system," *IEEE Access*, vol. 5, pp. 17869–17880, 2017.
- [18] Y. Liu, Z. Qin, M. Elkashlan, Z. Ding, A. Nallanathan, and L. Hanzo, "Nonorthogonal multiple access for 5G and beyond," *Proc. IEEE*, vol. 105, no. 12, pp. 2347–2381, Dec. 2017.
- [19] G. Gui, H. Huang, Y. Song, and H. Sari, "Deep learning for an effective nonorthogonal multiple access scheme," *IEEE Trans. Veh. Technol.*, vol. 67, no. 9, pp. 8440–8450, Sep. 2018.
- [20] Y. Wu, L. Qian, H. Mao, X. Yang, and X. Shen, "Optimal power allocation and scheduling for non-orthogonal multiple access relay-assisted networks," *IEEE Trans. Mobile Comput.*, vol. 17, no. 11, pp. 2591–2606, Nov. 2018.
- [21] P. Corcoran and S. K. Datta, "Mobile-edge computing and the Internet of Things for consumers: Extending cloud computing and services to the edge of the network," *IEEE Consum. Electron. Mag.*, vol. 5, no. 4, pp. 73–74, Oct. 2016.
- [22] X. Chen, Q. Shi, L. Yang, and J. Xu, "ThriftyEdge: Resource-efficient edge computing for intelligent IoT applications," *IEEE Netw.*, vol. 32, no. 1, pp. 61–65, Jan./Feb. 2018.
- [23] Q. Fan and N. Ansari, "Application aware workload allocation for edge computing-based IoT," *IEEE Internet Things J.*, vol. 5, no. 3, pp. 2146–2153, Jun. 2018.
- [24] F. Zhou, Y. Wu, H. Sun, and Z. Chu, "UAV-enabled mobile edge computing: Offloading optimization and trajectory design," in *Proc. IEEE ICC*, May 2018, pp. 1–6.
- [25] F. Zhou, Y. Wu, R. Q. Hu, and Y. Qian, "Computation rate maximization in UAV-enabled wireless-powered mobile-edge computing systems," *IEEE J. Sel. Areas Commun.*, vol. 36, no. 9, pp. 1927–1941, Sep. 2018.
- [26] L. Zhang, Z. Zhao, Q. Wu, H. Zhao, H. Xu, and X. Wu, "Energy-aware dynamic resource allocation in UAV assisted mobile edge computing over social Internet of vehicles," *IEEE Access*, vol. 6, pp. 56700–56715, 2018.
- [27] Q. Hu, Y. Cai, G. Yu, Z. Qin, M. Zhao, and G. Y. Li, "Joint offloading and trajectory design for UAV-enabled mobile edge computing systems," *IEEE Internet Things J.*, vol. 6, no. 2, pp. 1879–1892, Apr. 2019.
- [28] S. Jeong, O. Simeone, and J. Kang, "Mobile cloud computing with a UAV-mounted cloudlet: Optimal bit allocation for communication and computation," *IET Commun.*, vol. 11, no. 7, pp. 969–974, May 2017.
- [29] S. Jeong, O. Simeone, and J. Kang, "Mobile edge computing via a UAV-mounted cloudlet: Optimization of bit allocation and path planning," *IEEE Trans. Veh. Technol.*, vol. 67, no. 3, pp. 2049–2063, May 2018.
- [30] Y. Wu, L. P. Qian, K. Ni, C. Zhang, and X. Shen, "Delay-minimization nonorthogonal multiple access enabled multi-user mobile edge computation offloading," *IEEE J. Sel. Topics Signal Process.*, vol. 13, no. 3, pp. 392–407, Jun. 2019.
- [31] Y. Ai, L. Wang, B. Jiao, and K.-C. Chen, "Exploiting NOMA into socially enabled computation offloading," in *Proc. IEEE WCSP*, Dec. 2017, pp. 1–6.
- [32] A. Kiani and N. Ansari, "Edge computing aware NOMA for 5G networks," *IEEE Internet Things J.*, vol. 5, no. 2, pp. 1299–1306, Apr. 2018.
- [33] F. Wang, J. Xu, and Z. Ding, "Optimized multiuser computation offloading with multi-antenna NOMA," in *Proc. IEEE Globecom Workshops (GC Wkshps)*, Dec. 2017, pp. 1–7.
- [34] Y. Wu, K. Ni, C. Zhang, L. P. Qian, and D. H. K. Tsang, "NOMA-assisted multi-access mobile edge computing: A joint optimization of computation offloading and time allocation," *IEEE Trans. Veh. Technol.*, vol. 67, no. 12, pp. 12244–12258, Dec. 2018.
- [35] J. Du, L. Zhao, J. Feng, and X. Chu, "Computation offloading and resource allocation in mixed fog/cloud computing systems with min-max fairness guarantee," *IEEE Trans. Commun.*, vol. 66, no. 4, pp. 1594–1608, Apr. 2018.
- [36] M. Grant and S. Boyd. (Sep. 2013). *CVX: Matlab Software for Disciplined Convex Programming, Version 2.0 Beta*. [Online]. Available: <http://cvxr.com/cvx>
- [37] D. Zhang, Z. Chen, M. K. Awad, N. Zhang, H. Zhou, and X. S. Shen, "Utility-optimal resource management and allocation algorithm for energy harvesting cognitive radio sensor networks," *IEEE J. Sel. Areas Commun.*, vol. 34, no. 12, pp. 3552–3565, Dec. 2016.

- [38] S. Boyd and L. Vandenberghe, *Convex Optimization*. Cambridge, U.K.: Cambridge Univ. Press, 2004.
- [39] J. Xu, Y. Zeng, and R. Zhang, "UAV-enabled wireless power transfer: Trajectory design and energy optimization," *IEEE Trans. Wireless Commun.*, vol. 17, no. 8, pp. 5092–5106, Aug. 2018.
- [40] M. F. Sohail, C. Y. Leow, and S. Won, "Non-orthogonal multiple access for unmanned aerial vehicle assisted communication," *IEEE Access*, vol. 6, pp. 22716–22727, 2018.
- [41] N. Zhao, X. Pang, Z. Li, Y. Chen, F. Li, Z. Ding, and M.-S. Alouini, "Joint trajectory and precoding optimization for UAV-assisted NOMA networks," *IEEE Trans. Commun.*, vol. 67, no. 5, pp. 3723–3735, May 2019.
- [42] C. Guo, B. Liao, L. Huang, Q. Li, and X. Lin, "Convexity of fairness-aware resource allocation in wireless powered communication networks," *IEEE Commun. Lett.*, vol. 20, no. 3, pp. 474–477, Mar. 2016.
- [43] F. Cheng, S. Zhang, Z. Li, Y. Chen, N. Zhao, F. R. Yu, and V. C. M. Leung, "UAV trajectory optimization for data offloading at the edge of multiple cells," *IEEE Trans. Veh. Technol.*, vol. 67, no. 7, pp. 6732–6736, Jul. 2018.
- [44] S. D. Muruganathan, X. Lin, H.-L. Maattanen, J. Sedin, Z. Zou, W. A. Hapsari, and S. Yasukawa, "An overview of 3GPP release-15 study on enhanced LTE support for connected drones," 2018, *arXiv:1805.00826*. [Online]. Available: <https://arxiv.org/abs/1805.00826>
- [45] J. Zheng, Y. Cai, Y. Liu, Y. Xu, B. Duan, and X. Shen, "Optimal power allocation and user scheduling in multicell networks: Base station cooperation using a game-theoretic approach," *IEEE Trans. Wireless Commun.*, vol. 13, no. 12, pp. 6928–6942, Dec. 2014.



XIANBANG DIAO received the B.S. degree in communication engineering from Chongqing University, Chongqing, China, in 2017. He is currently pursuing the M.S. degree with the College of Communication Engineering, Army Engineering University of PLA. His current research interests include mobile edge computing, interference mitigation techniques, and optimization techniques.



JIANCHAO ZHENG received the B.S. degree in communications engineering and the Ph.D. degree in communications and information systems from the College of Communications Engineering, PLA University of Science and Technology, Nanjing, China, in 2010 and 2016, respectively. From 2015 to 2016, he was a Visiting Scholar with the Department of Electrical and Computer Engineering, Broad-band Communications Research Group, University of Waterloo, Canada. He was an Assistant Professor with the College of Communications Engineering, Army Engineering University of PLA. He is currently an Assistant Professor with the National Innovation Institute of Defense Technology, Academy of Military Sciences of PLA. He has authored or coauthored several papers in international conferences and reputed journals in his research area. His research interests include interference mitigation techniques, green communications and computing networks, game theory, learning theory, and optimization techniques.



YUAN WU (S'08–M'10–SM'16) received the Ph.D. degree in electronic and computer engineering from the Hong Kong University of Science and Technology, Hong Kong, in 2010. He is currently an Associate Professor with the State Key Laboratory of Internet of Things for Smart City, and also with the Department of Computer and Information Science, University of Macau. Prior to that, he was a Full Professor with the College of Information Engineering, Zhejiang University of Technology, China. His research interests include resource management for wireless networks, green communications and computing, mobile edge computing, and smart grids. He was a recipient of the Best Paper Award from the IEEE International Conference on Communications, in 2016, and the IEEE Technical Committee on Green Communications and Computing, in 2017.



YUEMING CAI received the B.S. degree in physics from Xiamen University, Xiamen, China, in 1982, and the M.S. degree in micro-electronics engineering and the Ph.D. degree in communications and information systems from Southeast University, Nanjing, China, in 1988 and 1996, respectively. He is currently a Full Professor with the College of Communications Engineering, Army Engineering University of PLA. His current research interest includes cooperative communications, signal processing in communications, wireless sensor networks, and physical layer security.



ALAGAN ANPALAGAN (S'98–M'01–SM'04) received the B.A.Sc., M.A.Sc., and Ph.D. degrees in electrical engineering from the University of Toronto, Canada. He joined the ELCE Department, Ryerson University, Canada, in 2001. He was promoted to a Full Professor, in 2010. He was with the department in administrative positions as the associate chair, the program director of electrical engineering, and the graduate program director. During his sabbatical leave, he was a Visiting Professor with the Asian Institute of Technology and a Visiting Researcher with Kyoto University. His industrial experience includes working for three years with Bell Mobility, Nortel Networks, and IBM. He is the Director of a research group working on radio resource management (RRM) and radio access and networking (RAN) areas within the WINCORE Laboratory. He has coauthored four edited books and two books in wireless communication and networking areas. He is a fellow of the Institution of Engineering and Technology (FIET) and the Engineering Institute of Canada (FEIC). He was a recipient of the Deans Teaching Award, in 2011, the YSGS Outstanding Contribution to Graduate Education Award, in 2017, the IEEE Canada J. M. Ham Outstanding Engineering Educator Award, in 2018, and the Faculty Scholastic, Research and Creativity Award thrice from Ryerson University. He was also a recipient of the Exemplary Editor Award from the IEEE ComSoc, in 2013, the IEEE M.B. Broughton Central Canada Service Award, in 2016. He was the Editor-in-Chief of the Top10 Choice Award of *Transactions on Emerging Telecommunications Technology*, in 2012. He has coauthored a paper that received the IEEE SPS Young Author Best Paper Award, in 2015. He is a Registered Professional Engineer in the province of Ontario, Canada. He has served as the TPC Co-Chair for the IEEE VTC Fall 2017, and the TPC Co-Chair for the IEEE INFOCOM 2016: Workshop on Green and Sustainable Networking and Computing, the IEEE GLOBECOM 2015: SAC Green Communication and Computing, and the IEEE PIMRC 2011: Cognitive Radio and Spectrum Management. He served as the Vice Chair for the IEEE SIG on Green and Sustainable Networking and Computing with Cognition and Cooperation, from 2015 to 2018, the IEEE Canada Central Area Chair, from 2012 to 2014, the IEEE Toronto Section Chair, from 2006 to 2007, the ComSoc Toronto Chapter Chair, from 2004 to 2005, and the IEEE Canada Professional Activities Committee Chair from 2009 to 2011. He has served as an Editor for the *EURASIP Journal of Wireless Communications and Networking*, from 2004 to 2009, the IEEE COMMUNICATIONS LETTERS, from 2010 to 2013, and the IEEE COMMUNICATIONS SURVEYS AND TUTORIALS, from 2012 to 2014. He also served as a Guest Editor for six special issues published in the IEEE, IET, and ACM.

...